communications chemistry

A Nature Portfolio journal

Article

https://doi.org/10.1038/s42004-025-01692-y

Relationship between ices and gas phase organic compounds in simulated extraterrestrial environments

Thomas Javelle[1], Fabrice Duvernay[1], Alexander Ruf[2,3], Chloé Granjon[1], Laura Selliez[4] & Grégoire Danger[1,5]

Ices are significant sources of organic matter in various extraterrestrial environments, including the interstellar medium, protoplanetary disks, comets, or icy satellites. This study tested the impact of ice compositions on the formation of volatile organic compounds (VOCs) in the gas phase in simulating the warming up of photoprocessed icy grains at the edge of a protoplanetary disk. 39 VOCs (alkanes, alkenes, esters, ketones, ethers, alcohols, aldehydes, amines, nitriles, amides) were quantified during the warming of different H_2O:CH_3OH:NH_3 ices using gas chromatography coupled to high-resolution mass linked to a vacuum chamber. Different ice compositions showed direct relationships to VOC formation processes and unveiled the active role of NH_3 reactivity. These results indicate that quantifying VOCs in the gas phase could provide insights into composition and surface reactivity of icy extraterrestrial objects. This experimental work further strengths the role that ices play in the enrichment of gas phase of various extraterrestrial environments.

Organic matter is found in various astrophysical environments, and a wide diversity is observed, depending on specific conditions and the analytical instruments used for the observation. Gas phase observations have revealed a high molecular diversity in different environments using submillimeter telescopes, such as ALMA[1,2]. To probe the surfaces of objects, infrared telescopes are often employed, such as ISO or the most recent JWST[3,4]. They provide information on chemical functions, but are still limited in obtaining full information on the large range of potential compounds present in such environments.

Space missions have developed various analytical systems to perform in situ analyses, offering complementary information to telescope observations. For instance, the Rosetta space mission has provided significant insights to understand the gaseous environment of the 67 P/Churyumov-Gerasimenko comet. Mass spectrometry[5] analyses provided evidence for various organic compounds, including the simplest amino acid, glycine[6]. Using the VIRTIS infrared spectrometer, the first details about the surface of this comet were obtained, suggesting the presence of ammonium salts[7].

However, information about the molecular diversity remains sparse, even with in situ analyses. Consequently, other space missions have developed an alternative approach aiming at returning samples from the targeted objects. The Stardust mission, for example, returned samples from the coma of the 81 P/Wild comet[8–10]. Recent Hayabusa 2 mission returned samples from a carbonaceous asteroid, Ryugu[11]. The most powerful ground-based analytical systems were used to analyze the organic content of these samples, revealing the high molecular diversity present on the surface of such interplanetary objects[12,13]. Interestingly, these analyses confirmed previous findings of organics in meteorites without the risk of contamination[14].

To deepen our understanding of the chemistry occurring in such astrophysical objects, laboratory experiments are crucial. Constrained by observations, these experiments simulate specific extraterrestrial environments. Among them, experiments on icy environments have demonstrated the potential to generate significant molecular diversity when exposed to UV photons, electrons, or ions[15–18]. For instance, ices composed of H_2O, CO, CO_2, CH_3OH, and NH_3 formed at 20 K, considered as interstellar ice analogs in dense molecular cloud ices, once altered, exhibit a chemical network containing thousands of different compounds[19]. At room temperature, in the remaining refractory residue, tens of thousands of distinct organic molecules have been observed in the resulting solid phases, with masses up to 4000 Da[20].

The chemistry occurring is mainly driven at low temperature by radical chemistry[21], while an additional thermal reactivity occurs during the warming processes[22]. Studies on the variation of ice composition have demonstrated its effect on the final solid organic samples[23]. Competition between carbon and nitrogen sources has been observed, leading to various

---

[1]Aix-Marseille Université, CNRS, Laboratoire PIIM, Marseille, France. [2]LMU Munich, Faculty of Physics, Munich, Germany. [3]Excellence Cluster ORIGINS, Garching, Germany. [4]LPC2E, OSUC, Univ Orleans, CNRS, CNES, Orleans, France. [5]Institut Universitaire de France (IUF), Paris, France.
e-mail: gregoire.danger@univ-amu.fr

chemical families observed in the resulting organic solid phases. Furthermore, H_2O exhibits a significant effect on reactivity by maintaining molecules at temperatures higher than their desorption temperatures, thereby facilitating their reactivity during the ice warming[24].

In addition to analyzing the solid organic phases, other experiments have been developed to characterize volatile organic compounds (VOCs) potentially released in the gas phase during the warming of photoprocessed ice. Initial experiments on pure methanol ices irradiated with UV photons at Lyman α have demonstrated the release of a wide range of organic molecules[25–27]. Interestingly, the abundance of molecules in the gaseous phase aligns with the radical chemistry proposed to occur during molecular formation[27]. Furthermore, the large range of compounds observed in the gas phase depends on photon dose and temperature[28].

Regarding the gas phase, the influence of the ice composition on the nature and the abundance of organic molecules released[23] has been investigated. Focusing only on molecules with oxygen, carbon, and hydrogen (CHO molecules), studies have shown how doping methanol ice with H_2O and NH_3 impacts the abundance of six volatile organic compounds (VOCs): one ether, four aldehydes, and one alcohol initially produced from pure methanol ice. The effects of adding H_2O or NH_3 significantly vary, depending on the chemical family. For example, adding water to methanol ice increases the abundance of aldehydes detected in the gas phase, while it inhibits ether formation[23].

In this study, we explore how the ice composition of dense molecular clouds can affect the type and the abundance of VOCs released into the gas phase after warming up photoprocessed ices. Specifically, we investigated ternary ices consisting of varying molecular ratios of H_2O, CH_3OH, and NH_3. VOCs were analyzed using Gas Chromatography coupled with High-Resolution Fourier Transform Mass Spectrometry (GC-FT-Orbitrap-MS). This analytical system allowed to identify 24 VOCs, including alkanes, alcohols, aldehydes, alkenes, amines, ethers, esters, ketones, and nitriles. In addition, due to the high-resolution capabilities of the mass spectrometry, we detected 15 other compounds based on their stoichiometric formulas without direct identification. We obtained insights into how ice compositions influence 39 different VOCs detected in the gas phase. This provides new insights into the role of astrophysical ices in the enrichment of the gas phase with VOCs.

Results

Volatile organic compounds analyzed with GC-FT-Orbitrap-MS

Figure 1 depicts chromatograms of volatile organic compounds (VOCs) detected in the sublimated gas-phase mixture after warming the photoprocessed ice samples to 300 K. We studied four different compositions of ice containing H_2O:CH_3OH:NH_3 (Table 1): a benchmark (3:1:2), H_2O-rich (8:1:2), NH_3-rich (2:1:5), and CH_3OH-rich (2:5:3). As shown in Fig. 1, the overall intensities of detected VOCs are influenced by the initial ice composition. The highest intensities are observed with an excess of CH_3OH, while the lowest intensities are observed with an excess of NH_3. Therefore, the ice composition directly affects the branching ratios within the ice during both its photo-processing and subsequent warming phases.

Using retention times and fragmentation patterns of each peak, tentative identifications of volatile organic compounds (VOCs) were performed by comparing these data to our database containing 150 VOCs. Among the signals observed, 24 compounds were unequivocally identified, including ethers, aldehydes, ketones, hydrocarbons, esters, amines, alkenes, alkanes, and nitriles (Fig. 2 and Table S1). Additionally, many signals remained unidentified. Since a high-resolution mass spectrometer (resolution 60,000 at *m/z* 200) was operated, stoichiometric formulas were assigned to each ion in a fragmentation pattern, providing valuable information about their chemical composition (CH, CHO, CHN, CHNO) and degree of unsaturation (double bond equivalents, *DBE*). This approach yielded additional insights into the chemical groups of 15 other VOCs (Fig. 2 and Table S1). Overall, our study encompassed 39 different VOCs, spanning all chemical groups and families analyzable with our GC-FT-Orbitrap-MS protocol.

Effect of ice composition on abundances of volatile organic compounds

Evolution of identified compounds. To assess the impact of the initial ice compositions on abundances of the VOCs produced (Fig. 1), we compared our benchmark experiment (3:1:2) with other compositions (H_2O-rich 8:1:2, NH_3-rich 2:1:5, and CH_3COH-rich 2:5:3) for all identified compounds categorized by their chemical functions (as shown in Fig. 2). In the text, only absolute abundances are discussed, since same evolution are observed if relative abundances to the quantity of deposited

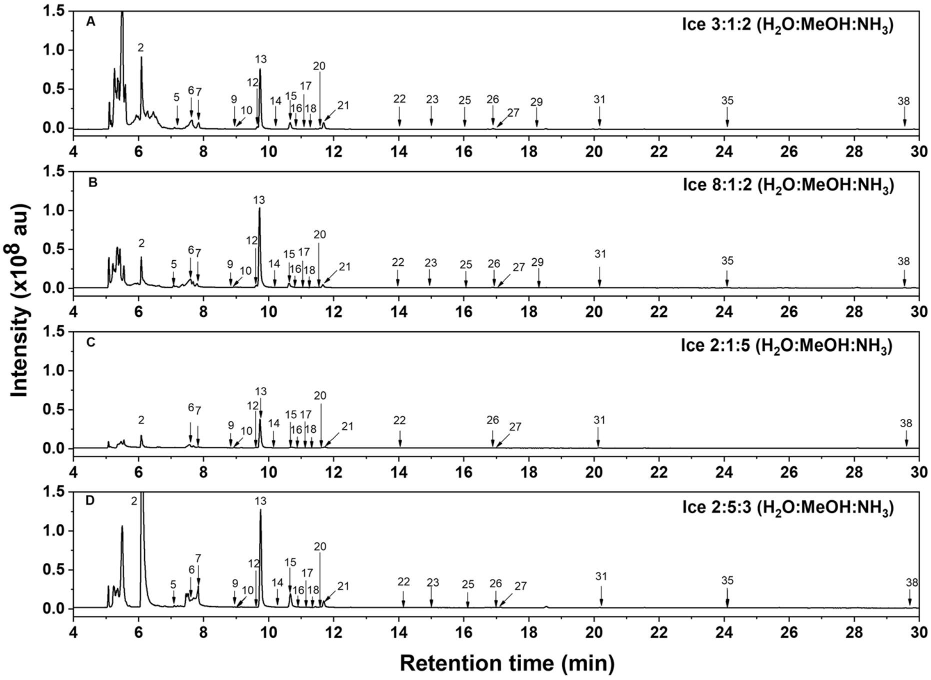

Fig. 1 | Chromatograms observed from GC-FT-Orbitrap-MS analyses. Chromatograms corresponding to H_2O:CH_3OH:NH_3 ices in the proportions 3:1:2 (**A**); 8:1:2 (**B**); 2:1:5 (**C**), and 2:5:3 (**D**). The number refers to VOCs identified with a standard (Table S1). Tentative assignments are not notes in the chromatograms.

Table 1 | Composition of ice samples and the corresponding apparent irradiation rate relative to CH_3OH used in this work

Ices	$H_2O:CH_3OH:NH_3$	Total deposition (× 10^{18} H_2O molecules)	Total deposition (× 10^{18} CH_3OH molecules)	Total deposition (× 10^{18} NH_3 molecules)	Deposition rate (× 10^{17} H_2O/h)	Deposition rate (× 10^{17} NH_3/h)	Deposition rate (× 10^{17} CH_3OH /h)	Irradiation time (h)	Apparent irradiation rate (photon/ CH_3OH)
Benchmark	3:1:2	6.6	2.4	4.1	4.0	2.5	1.5.10.10	5.50	15
H_2O-rich	8:1:2	19	2.5	5.7	11	3.4	1.5	5.50	14
NH_3-rich	2:1:5	5.3	3.4	18	3.2	11	2.1	5.50	11
CH_3OH-rich	2:5:3	1.4	3.7	2.5	0.8	1.5	2.2	5.50	10

Except for irradiation time, values accept up to 40% of error because of experimental variability. The Benchmark ice corresponds to the ice that is used as a reference in our laboratory to compare all our data[15,23].

CH_3OH are used (Fig. S19). Figure 3 presents one representative compound per chemical family, while Figs. S1 and S15 display trends for all detected compounds.

For alkanes (pentane #9) or alkenes (1-pentene #10), similar trends are observed (Figs. 3, S1 and S14). Higher amounts of CH_3OH, H_2O, or NH_3 in the ice increase the abundance of hydrocarbons (Figs. 3, S1 and S14), with a stronger effect observed with CH_3OH. However, for aromatic compounds (Fig. 3, benzene #31, and S1), trends differ. The abundance of these compounds decreases in NH_3-rich ice, while CH_3OH or H_2O-rich ices show a non-significant effect compared to the benchmark.

For alcohols (ethanol #12) or ethers (dimethylether #2), the most significant changes are observed in CH_3OH-rich ices (Figs. 3, S1 and S14), showing a strong increase in compound abundance. NH_3 and H_2O do not exhibit significant or observable effects in this context (Fig. 3). However, there is a notable difference with diethyl ether #13 (Fig. S1), which is weakly affected by the amount of H_2O, and moderately affected by the amount of CH_3OH. Regarding aldehyde (acetaldehyde #5) or ketones (acetone #15) compounds when increasing the amount of CH_3OH in the ice, their abundances slightly or moderately increase, except for 2-butanone #25, which shows a negative effect. In contrast, H_2O appears to have a significant positive influence on aldehydes compared to ketones (Figs. 3 and S1). The presence of NH_3 has a negative effect, resulting in a significant depletion for all compounds in this category. Notably, 2-butanone #25 was not observed in H_2O-rich ice conditions.

For saturated compounds bearing two oxygen chemical functions, two ethers (dimethoxy methane #16) or ether -alcohol (methoxymethanol #28), the same trend as described previously in the corresponding mono-functional groups is observed. For esters (methyl acetate #21), the situation is different. They all present the same evolution with an increase of their abundance in CH_3OH-rich ice, and depletions in the presence of higher amounts of H_2O and NH_3. One exception is observed with ethyl acetate #26, where CH_3OH inhibits its formation, H_2O has a weak positive effect and NH_3 still presents a negative influence.

Two amines were detected in the gas phase: ethylamine #14 and propylamine #34. Ethylamine is present in all samples. The overabundance of NH_3 in the ice has a strong positive effect on amine abundances compared to the benchmark ice. With H_2O and CH_3OH, the influence is still positive, but weaker. Propylamine is only visible in the ice enriched in NH_3, confirming the large increase observed with ethylamine. Two nitriles were identified: acetonitrile #20 and propionitrile #27. In this case, NH_3, unlike amines, inhibits their formation. CH_3OH and H_2O have only a weak influence.

Unidentified compounds. Among the 39 compounds detected in our experiments, 15 were not identified using a standard. Their mass spectra are shown in Fig. S16. Tentative identifications were investigated by taking advantage of the high resolution of the Orbitrap instrument, which provided stoichiometric formulas for each ion detected in the mass spectra, allowing us to assign them to a family group (CH, CHO, CHN or CHNO). Then, mass spectra were compared to a standard list and the NIST (National Institute of Standards and Technology) database to propose some identifications based on specific fragmentation patterns, providing structural information (for more details, see Supplementary Information). Corresponding assumptions are given in italics in Table S1. For 11 of these compounds, a specific compound is suggested, while for three of them, only a chemical group attribution was proposed.

Particularly, two compounds were attributed to CHNO compounds. Only monounsaturated CHNO compounds (Table S1) were detected, which does not correspond to the detection of alcoholamines that have already been identified in such ices[24,29]. Since no standards were available for the identification, it was difficult to determine the structure. However, if their fragmentation spectra are compared to those of amide compounds from the NIST database (Fig. S15), correlations are observed. Consequently, the CHNO compounds are probably acetamide (#4) and propylamide (#19). Their evolution shows similarities with aldehydes, ketones, and nitriles (Fig. S15). Compared to the benchmark ice, NH_3 has

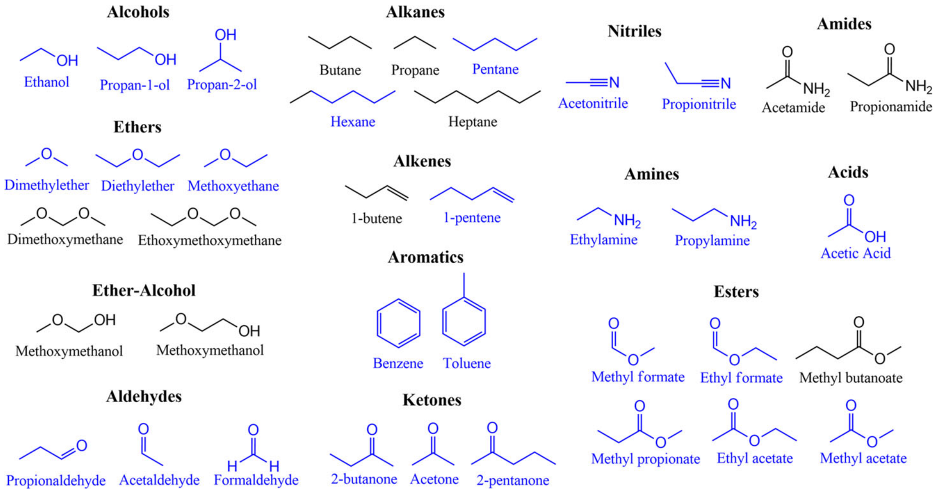

Fig. 2 | Volatile organic compounds detected during the different experiments with GC-FT-Obitrap analyses. In blue are the molecules identified with a standard, while in dark are the molecules tentatively identified. Additional information is displayed in Figs. S2–S16.

a strong negative effect, while CH_3OH and H_2O have positive influences (Fig. S15).

For unidentified hydrocarbons, investigations using their fragmentation spectra allowed for putative attributions to propane (#1), 1-butene (#3), butane (#9), and heptane (#33). Compared to identified compounds, they exhibit rather similar evolutions, except for propane, which shows an evolution similar to the alkene family.

Additional compounds carrying two oxygen were also tentatively identified as dimethoxymethane (#25), methoxymethanol (#28), and ethoxyethanol (#30), and probably an alcohol-ether (#38). Similar trends to CHO or compounds carrying two oxygen with DBE = 0 were observed, with a significant increase in their abundance in CH_3OH-rich ice and a depletion in NH_3-rich ice. Finally, a compound $C_6H_6O_2$ at 25.79 min (#37) with a DBE = 4 displays an evolution similar to CHO compounds with DBE = 0. Abundant evolutions of $C_6H_6O_2$ differ from aromatic compounds, such as toluene or benzene, which show a depletion in its abundance in CH_3OH-rich ice. At this stage, it is difficult to determine a precise structure except that the compound likely bears a hydroxyl moiety.

Discussion

In this work, ices composed of $CH_3OH:NH_3:H_2O$ are altered through VUV irradiation and a subsequent warming. These three molecules are among the main constituents ices detected in dense molecular clouds by infrared spectroscopy, as well as on interstellar grains[30]. We thus simulate the physical and chemical evolution that interstellar or circumstellar ices could undergo during the formation and development of a planetary system. This includes temperature conditions ranging from 10 to 100 K and photon fluxes varying from ~0 to 10^8 photons $cm^{-2}\ s^{-1}$, depending on the grain's location within the nebula[31].

In our experimental setup, the ice temperature is maintained at 78 K—representative of a grain located at the outer edge of a protoplanetary disk—and is exposed to a UV flux of 2×10^{14} photons $cm^{-2}\ s^{-1}$ (see ref. 31). After 44 h of simultaneous deposition and irradiation, the total UV dose reaches 3×10^{19} photons cm^{-2}, corresponding to the cumulative exposure of a grain would receive over 10^6 years in a disk environment at a flux of 10^6 photons $cm^{-2}\ s^{-1}$ (see ref. 31). The refractory residue obtained at the end of the experiment (under laboratory conditions of 300 K and 10^{-8} mbar) can thus be considered as a laboratory analog of the refractory organic materials that may exist on interstellar grains and could eventually be incorporated into comets or asteroids. Thousands of organic compounds are indeed observed in these refractory organic materials remaining on the sample holder[15,16]. These results highlight the importance of ice reactivity in the formation of organic matter in various astrophysical environments. Regarding the gas phase, several experiments have demonstrated that ice processing might also release volatile organic compounds into the gas phase[17,25,27,32,33]. In general, two main experimental methods are available to study ice reactivity under laboratory conditions. The first approach involves forming an ice layer that is subsequently irradiated. In contrast, the second approach consists of irradiating the sample during the ice formation process. These two methods simulate different astrophysical environments. In the second case, interactions between photons and gas-phase molecules are likely, which can mimic conditions near snowlines. This may lead to the formation of radicals both in the gas phase and within the growing ice. However, the synthesis of organic compounds generally requires higher molecular densities, which are more readily achieved in the solid phase than in the gas phase. Importantly, our current results are fully consistent with those obtained using the post-deposition irradiation method[28], reinforcing the conclusion that the observed COVs arise from chemical processes occurring within the ice rather than in the gas phase.

Most of the experiments on VOC generated from ices focused on the irradiation of pure methanol ices. Öberg et al. used temperature-programmed desorption coupled with a mass spectrometer to obtain information on VOCs released into the gas phase from a VUV-photoprocessed ice of methanol[25]. Coupled with infrared spectroscopy measurements of the photoprocessed ice, a preliminary reaction network was proposed to explain the formation of the observed compounds.

The reactivity of methanol is mainly based on radical formation, which recombines by diffusion in the ice to form the observed compounds[21]. The radical reactivity was later confirmed by the direct detection of radicals CH_3, CH_2OH, and HCO[34]. The effect of the VUV photon doses was also investigated using GC-MS. Quantification of VOCs in the gas phase provided additional information on the reactivity occurring during the ice processing[28]. In particular, it was demonstrated that ketones and esters form rapidly from CO, while aldehydes form from HCO, except for acetaldehyde, which forms from the photo-processing of ethanol[28,34]. Alcohols are species that form more slowly. Other experimental setups were designed to directly analyze VOCs in the gas phase using submillimeter spectroscopy[26].

If the ice composition is more diverse by adding water and/or ammonia, the number of chemical pathways and the molecular diversity increase in the solid phase[23,24,35]. The ratio of NH_3 to CH_3OH is particularly crucial, with nitrogen (N) and carbon (C) competing for the formation of the molecular skeleton[23,36]. Regarding the gas phase, initial analyses of the VOCs with GC-MS have shown that ice reactivity can be directly observed[23]. However, this initial experiment focused only on CHO compounds due to a lack of sensitivity. In this study, using a more sensitive analytical system, we were able to obtain data on other chemical groups: CH, CHO (with one or two O), CHN, and CHNO. These results provide new insights into the

Fig. 3 | Evolution of absolute intensities as a function of the ice composition for selected VOCs representative of their chemical family evolution. Ethanol #12: alcohols; dimethylether #2: ethers; acetaldehyde #5: aldehydes; methylacetate #21: esters; ethylamine #14: amines; acetonitrile #20: nitriles; benzene #31: aromatics; pentane #10: alkanes. Error bars were obtained from the average area measured on three repeated experiments.

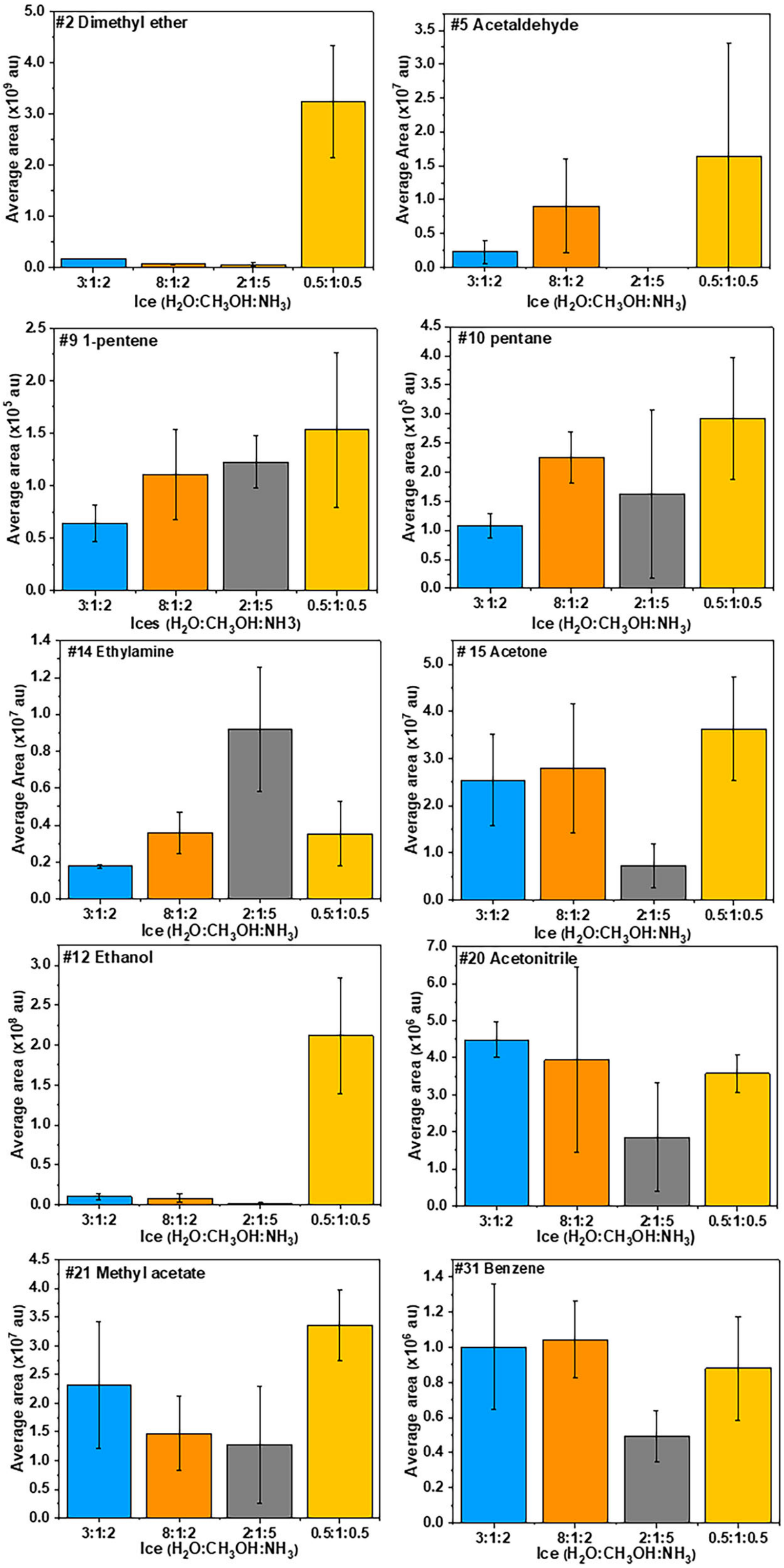

influence of ice composition on gas-phase VOCs sublimated from energetically processed ices, and indirectly on the low-temperature reactivity occurring in the ice once formed.

Reactivity leading to alkanes and alkenes

Alkanes and alkenes are mainly formed by the recombination of CH_3 radicals generated from the photodissociation of CH_3OH[34]. Even if ethane is not detectable with our analytical protocol, it can be assumed to form initially:

$$^{\cdot}CH_3 + {}^{\cdot}CH_3 \rightarrow C_2H_6 \tag{1}$$

From ethane, various alkanes, alkenes, and radicals can be formed, which explains the diversity of alkanes and alkenes observed[37–39]. It has to be noted that branched hydrocarbons were not yet identified. This could be due to analytical issues. Linear hydrocarbons are near their detection limit. Although branched hydrocarbons are thermodynamically more stable, branching ratios leading to these compounds could be different from linear hydrocarbons and led to different abundances. Their abundances may be lower than their linear part, thus being outside our detection limits. Additional investigations have to be performed to elucidate this aspect.

Reactivity leading to alcohols and ethers

As for alkanes, CH_3OH is the main precursor of the detected alcohols and ethers, as shown by its high positive effect on their abundances (Figs. 3, S1 and S14). As already discussed by Oberg et al.[25], they are formed by direct recombination of methanol radicals. For example, dimethylether is formed according to Eq. (2) and ethanol according to Eq. (3).

$$^{\cdot}CH_3 + {}^{\cdot}OCH_3 \rightarrow CH_3OCH_3 \tag{2}$$

$$^{\cdot}CH_3 + {}^{\cdot}CH_2OH \rightarrow CH_3CH_2OH \tag{3}$$

Alcohols with longer carbon chains can be formed from chain elongation of smaller alcohol via secondary and tertiary reactions, from the recombination of alkane and hydroxyl radicals or hydrogenation of their corresponding aldehydes[28,40]. Same mechanisms could lead to diethers, such as dimethoxymethane, which requires recombination (4) and (5)

$$CH_3OCH_3 + hv \rightarrow CH_3OCH_2^{\cdot} + H^{\cdot} \tag{4}$$

$$CH_3OCH_2^{\cdot} + {}^{\cdot}OCH_3 \rightarrow CH_3OCH_2OCH_3 \tag{5}$$

The influence of H_2O on the quantity of alcohol and ether are in total accordance with observation made in ternary ices by Abou Mrad et al.[27]. An increase in the amount of H_2O inhibits the formation of alcohols and ethers. The mechanism proposed to explain this phenomenon was the availability of $H^{\bullet}$ radicals favoring recombination with $CH_3O^{\bullet}$, thereby reducing the abundance of this radical.

A moderate negative effect of NH_3 is observed for both families. This can be explained by the formation of the amino radical $^{\bullet}NH_2$ generated by the photodissociation of NH_3 (6)[41,42] that recombines with alkane precursors ($^{\bullet}C_xH_y$) (7), decreasing their availability to lead to alcohol and ether formation.

$$NH_3 + hv \rightarrow {}^{\cdot}NH_2 \tag{6}$$

$$^{\cdot}NH_2 + {}^{\cdot}C_xH_y \rightarrow NH_2C_xH_y \tag{7}$$

Reactivity leading to aldehydes and ketones

In the case of aldehydes, two different mechanisms are involved in their formation. In the case of acetaldehyde, a dehydrogenation of the corresponding alcohol is suggested (7)[28,34], while for others aldehydes, a recombination between the corresponding alkyl radical $R^{\bullet}$ and $HCO^{\bullet}$ (8 and 9) can explain their formation[28].

$$CH_3CH_2OH + hv \rightarrow CH_3CHO + H_2, \tag{7}$$

$$H_2CO + hv \rightarrow HCO^{\cdot} + H^{\cdot} \tag{8}$$

$$HCO^{\cdot} + R^{\cdot} \rightarrow HCOR \tag{9}$$

It was indeed shown that in pure CH_3OH ice, aldehydes are formed before their corresponding alcohol[28], at the difference of acetaldehyde. The recombination of HCO and $^{\bullet}CH_3$ that could lead to acetaldehyde, should form CH_4 and CO in pure CH_3OH[34,43,44]. However, in the presence of H_2O and NH_3 in the ice, the existence of this second pathway of aldehyde formation seems to be favored. Indeed, while no effect of H_2O is observed on ethanol formation, an important increase of acetaldehyde production is observed, confirming the first experiment on ternary ices[27]. If acetaldehyde was formed from ethanol, the same trend between both compounds should have been observed. Even if this observation does not rule out the first pathway, ethanol dehydrogenation alone cannot explain it. In fact, the presence of H_2O in the ice increases the abundance of $HCO^{\bullet}$ (10, 11, 12), which is consistent with the increase of the 1854 cm^{-1} band attributed to $HCO^{\bullet}$ in the presence of a higher amount of water in the ice (Table S2). This supports previous observations recorded for other aldehydes[28,45,46].

$$OH^{\cdot} + OH^{\cdot} \rightarrow H_2O_2 \tag{10}$$

$$^{\cdot}CH_2OH + H_2O_2 \rightarrow H_2CO + H_2O + {}^{\cdot}OH \tag{11}$$

$$H_2CO + hv \rightarrow HCO^{\cdot} + H^{\cdot} \tag{12}$$

The effect of the initial ice composition is different for ketones. Their formation occurs according to the mechanism (13) and (14), taking the example of the formation of acetone proposed by Tenelanda-Osorio et al.[28], consistent with the influence of H_2O and CH_3OH observed.

$$CO + {}^{\cdot}CH_3 \rightarrow CH_3CO^{\cdot} \tag{13}$$

$$CH_3CO^{\cdot} + {}^{\cdot}CH_3 \rightarrow CH_3(CO)CH_3 \tag{14}$$

NH_3 has the strongest negative effect on aldehyde and ketone formation, corroborating the first observation on acetaldehyde[27]. As for other families, NH_2 radical probably inhibited the availability of alkane chains (7), but mainly of CO or $HCO^{\bullet}$ by reacting with their radical precursor $^{\bullet}CH_2OH$ (15) or directly on $HCO^{\bullet}$ (16), consistent with the amide detection[27]. NH_3 could also react with H_2O_2[47], depleting formaldehyde formation (11) and indirectly $HCO^{\bullet}$ (12).

$$CH_3CO^{\cdot} + {}^{\cdot}NH_2 \rightarrow CH_3(CO)NH_2 \tag{15}$$

$$HCO^{\cdot} + {}^{\cdot}NH_2 \rightarrow H(CO)NH_2 \tag{16}$$

Reactivity leading to esters

Esters formate are suggested to form from the recombination of $HCO^{\bullet}$ with the corresponding alkoxy group (17)[25,34,48,49]. For other esters whose acyl groups contain a longer carbon chain, a two-step mechanism can be considered: starting from the reaction between an alkyl radical and CO (13) to form the acyl group, followed by the recombination of this acyl group with an alkoxy radical (18)[25,28,34,48,49].

$$HCO^{\cdot} + {}^{\cdot}OCH_3 \rightarrow HCOOCH_3 \tag{17}$$

$$CH_3CO^{\cdot} + {}^{\cdot}OCH_3 \rightarrow CH_3COOCH_3 \tag{18}$$

These mechanisms clearly explain the difference observed in the various ices between the abundances of methyl esters and esters formate, and the abundances of ethyl acetate. Methyl esters and ester formate are formed from primary radicals directly originating from the methanol photolysis. Their formation is favored by the increase of the methanol quantity initially present in the ice, to the detriment of ethyl acetate, which requires precursors coming from a more diverse reactivity and implying alkyl and alkoxy radicals of longer carbon chain.

It is also interesting to compare the evolution of aldehyde and esters formate, since they are suggested to form both from $HCO^{\bullet}$. However, regarding to the ice composition, they do not follow the same trend. Aldehydes present similarities with the evolution of alkanes, while esters formate follow the trend of alcohols. These observations are consistent as their formation is not depending on $HCO^{\bullet}$ (shared between both chemical families) but on other radicals. Therefore, their abundance differences rely

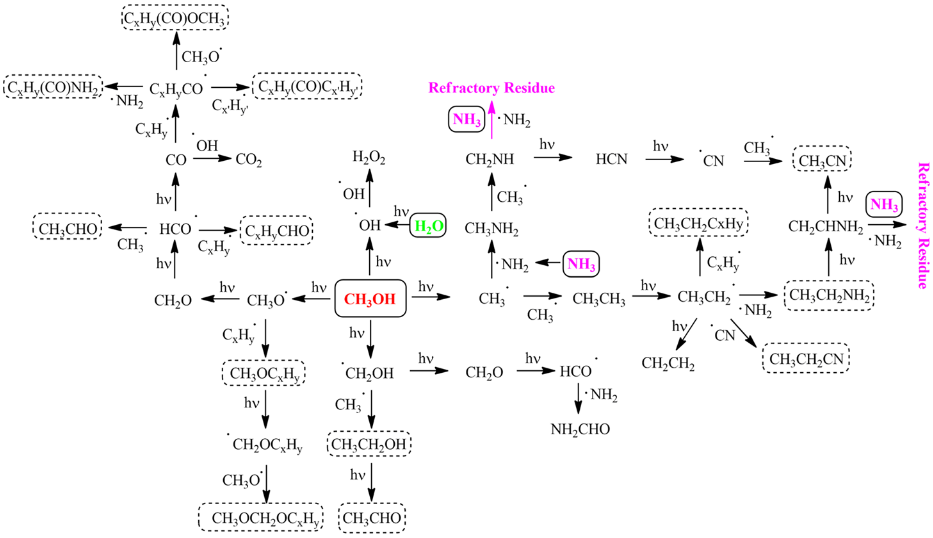

Fig. 4 | Ice reactivity explaining VOCs formation. Scheme presenting the reactivity possibly occurring in the icy phase after its photo-processing and warming, highlighting by the analysis of volatile organic compounds in the gas phase.

on the relative availability of alkyl for aldehydes, and alkoxy radicals for esters formate. As observed for alkanes and alcohols, these radicals do not present same trends for a same ice composition. The same observation can be made for ketones and methyl esters.

Finally, a strong decrease of their abundances is observed with a high abundance of NH_3 in the ice. Same reactivity as discussed for aldehydes and ketones could explain this behavior, meaning a consumption of radical precursors by NH_2 radical (7, 15, 16).

Reactivity leading to amines and nitriles

One of the most surprising results of this study is the antagonistic effect of the initial composition of the ice on the abundance of amines and nitriles. If the increase in the quantity of CH_3OH and H_2O is insignificant for these two chemical families, the quantity of NH_3 significantly increases the abundance of amines, while strongly decreasing the formation of nitriles.

For the amine formation, several mechanisms are proposed[50]. One way is using the hydrogenation of hydrogen cyanide (19)[51], or directly by ion-molecule reaction (20) then (21).

$$HCN + 4H^{\cdot} \rightarrow CH_3NH_2 \tag{19}$$

$$NH_3 + CH_3^+ \rightarrow CH_3NH_3^+ \tag{20}$$

$$CH_3NH_3^+ + hv \rightarrow CH_3NH_2 + H^+ \tag{21}$$

However, regarding the evolution of amine as a function of the ice composition, it seems that the main route in our operating conditions is the direct recombination of $^{\cdot}CxHy$ and $^{\cdot}NH_2$ radicals (22)[52], confirmed by the great increase of their abundances in NH_3-rich ices.

$$^{\cdot}C_2H_5 + {}^{\cdot}NH_2 \rightarrow C_2H_5NH_2 \tag{22}$$

Nitriles are proposed to be formed directly from the photo-processing of their corresponding amines (23–25), with imines as intermediates[53].

$$^{\cdot}NH_2 + C_2H_5^{\cdot} \rightarrow C_2H_5NH_2 \tag{23}$$

$$C_2H_5NH_2 + hv \rightarrow CH_3CH = NH + 2H \tag{24}$$

$$CH_3CH = NH + hv \rightarrow CH_3CN + 2H \tag{25}$$

However, the antagonist evolution of amines and nitriles in NH_3-rich ice implies that a side reaction occurs consuming nitrile precursors, inhibiting nitrile formation. Indeed, if such, a correlation between amine and nitrile formations should occur. Here, a clear abundance decrease of nitriles is observed, in the same sense as observed with other oxidized chemical families (aldehydes, ketones, esters). In fact, $^{\cdot}NH_2$ radical consumes a large part of the first generation of methanol radicals ($^{\cdot}CH_3$, $^{\cdot}CH_2OH$, $^{\cdot}OH$) precursors to form amine compounds, opening a competitive reactivity to the formation of CHO compounds (Fig. 4). This explains the high increase of amines with enriched NH_3 ice. Once amine, such as methylamine or ethylamine, are formed, irradiation probably leads to their corresponding imine (24), first step toward the formation of nitrile compounds (25). However, imines are highly reactive in our experimental conditions[54–57]. They easily react with $^{\cdot}NH_2$, NH_3, HCOOH or $^{\cdot}CN/^{-}CN$ to give refractory macromolecules that are part of the remaining organic residues formed after the photoprocessed ice warming. Consequently, a higher amount of nitrogen is incorporated in organic residue before nitrile formation, providing to a lower abundance of nitriles observed in the gas phase, since their imine precursors are trapped in refractory macromolecules.

This scenario is in total accordance with the previous experiment focused on the influences of ice composition on residue composition, showing that an increase of NH_3 in the ice can lead to an increase of its nitrogen content[23]. It is also supported by the decrease of all carbonyl compounds observed in the gas phase in NH_3-rich ice, corroborated by the decrease of the higher generation of methanol photoproducts, as observed with infrared spectroscopy (CO_2, NCO^-, CO, HCO, H_2CO, Table S2 and Fig. S7).

Reactivity leading to amides

The two detected amides, acetamide and propionamide, have roughly the same evolution as ketones. They present a higher positive effect with H_2O, a claim supported by previous results showing that H_2O increases nitrogen incorporation into compounds[17,18,23]. A negative effect of NH_3 is also explained by the decrease of CO formation, since their formation is based on the same precursors as ketones (13, 14), strengthening their identification as amides. An alternative formation pathway would be the direct incorporation of H_2O in nitriles. However, no correlation was observed between evolutions of nitriles and amides, specifically in the presence of a higher amount of H_2O that implies a decrease of nitriles, while amides increase. If a correlation would exist, a same trend should be observed, or a stronger decrease of nitriles in correlation with the amide increase observed, which is not the case.

Figure 4 summarizes the reactivity in the solid phase that possibly leads to the VOCs identified in the gas phase with our GC-FT-Orbitrap-MS.

These results demonstrate that the abundances of volatile organic compounds detected in the gas phase can be correlated with the chemistry occurring in the ice.

Even if further developments have to be performed to estimate the accuracy of using the gas phase as a probe of the surface composition, our current observations corroborate initial experiments focused on CHO compounds, confirming that H_2O plays a trapping role. Interestingly, by identifying nitrogen compounds, we gained insights into the role of NH_3 in the reactivity, and can directly connect gas phase abundance of VOCs to reactivity leading to refractory residue.

It appears that once the NH_3 proportion in the ice is high, an important competition occurs with carbonyl compounds (Table S2). It limits the precursor formation of aldehydes, ketones, and esters in the ice, reducing their abundances, as well as for nitriles. A CH_3OH increase gives an increase of VOC abundance. All these observations are consistent with the organic content of residues that are formed at room temperature after the warming up of the photoprocessed ices[15,23,58]. It was indeed demonstrated that an increase of H_2O in the ice leads to an increase of nitrogen incorporation in organic residues in the same sense as it is observed in the gas phase. The same observation was made about the amines detected in the gas phase. Furthermore, it was shown that a higher NH_3 content in the ice leads to an increase of nitrogen incorporation, which is intuitive, but with a decrease in the average DBE[23]. This is in agreement with our gas phase observation, where a higher amount of NH_3 leads to the detection of higher abundances of saturated compounds (ethylamine and propylamine), while unsaturated compounds in the gas phase present a decrease of their abundances due to the incorporation of their precursor (imines, ketenimines) in refractory residues.

Consequently, probing the gas phase may give information on the composition of the surface of icy environments, by taking into account the ratio between chemical families observed in the gas phase. This approach may be used in a near future to analyze observations in various astrophysical environments such as hot cores, protoplanetary disks or cometary environments.

Conclusion

Ice in extraterrestrial environments are known to be an important source of organic matter in various environments. In this contribution, we evaluate ices as a possible source of organics in the gas phase. Using gas chromatography coupled to a high-resolution mass spectrometry linked to a vacuum chamber, 24 volatile organic compounds were detected in the sublimated gas phase mixture, and tentatively identified 15 additional VOCs, including alkane, alkene, ester, ketone, ether, alcohol, aldehyde, and to the best of our knowledge, for the first time amine, nitrile and amide compounds, as well as some bifunctional compounds. Abundances of these VOCs were monitored depending on ice compositions to obtain a complete scheme of the reactivity leading to their formation. Furthermore, variation of molecular ratios in the initial ice provided information on VOCs formation. Particularly, in our operational conditions, NH_3 tends to compete with carbonyl compound formation and drive the formation nitrogen refractory compounds. Finally, all observations of VOCs evolution are directly explained by the reactivity occurring in the ice during its formation and photo-processing. It thus appears that ice can be an important reservoir of VOCs that can be released in the gas phase once in a warmer zone. Furthermore, the quantification of VOCs in the gas phase could give indirect information on the composition and reactivity occurring on the surface of an icy astrophysical object. Finally, this experimental work demonstrates the necessity to correlate ALMA observations giving information on the gas phase with the ones of JWST focusing on solid phase observations. By coupling these observations to the present work, information could be obtained to better understand the role of ices in VOCs observed in gas phases.

Methods

Ice photo-processing and volatile organic compounds recovery

The experimental setup for the synthesis of interstellar analogs is described in detail in refs. 59–61. Briefly, it is composed of a sample holder holding a MgF_2 window in a vacuum chamber (2.10^{-7} to 8.10^{-8} mbar). The sample holder where the ice is formed is set at 77 K using liquid nitrogen (Linde). The gas deposition for the ice formation is performed at the same time as the irradiation using an H_2 discharge lamp with continuous flow at 5 mbar (Lyman α, 121 nm, (3.7 ± 0.6).10^{14} photon*cm^{-2}*s^{-1}). A small contribution is also present at 160 nm. As previously described in Danger el al.[15] These conditions simulate an environment near the CO snowline, where condensation on grain can occur, while the UV photon flux is still abundant. Furthermore, during this process, photodissociation of H_2O, CH_3OH, and NH_3 in the gas phase probably occurs as well as in the ice phase, since the photodissociation cross section is higher in the gas phase[21]. Consequently, radical precursors can have these two origins, while organic molecules observed are formed in the icy phase[32]. The photon flux was calibrated using replicated actinometry on a methanol ice irradiation, monitoring the CO band of methanol (1047–1006 cm^{-1}: (1.8 ± 0.4).10^{-17} cm*molecule^{-1})[62]. Gas mixtures for ice formation were prepared in a reservoir with different proportions of H_2O (purified with a Millipore Direct Q5 system), CH_3OH (prepared from Fisher Chemicals, 99.99%) and NH_3 (purchased from AlphagazTM, 99.98%). The deposition rates and the molecular compositions of ice are estimated during the first hour of experiments and without the UV irradiation using a BRUKER Vector 22 FTIR Spectrometer in transmission mode (20 scans from 960 to 4000 cm^{-1} with 2 cm^{-1} of resolution and 400 scans of background). The following band strengths were used for each ice species H_2O (3612–3003 cm^{-1}: 2.10^{-16} cm*molecule^{-1}), CH_3OH (1047–1006 cm^{-1}: (1.8 ± 0.4).10^{-17} cm*molecule^{-}, 3612–3003 cm^{-1}: (1.0 ± 0.2).10^{-16} cm* molecule^{-1}) and NH_3 (^{1}1192 –1084 cm^{-1}: (1.6 ± 0.3).10^{-17} cm* molecule^{-1}, 3612–3003 cm^{-1}: (2.3 ± 0.5).10^{-17} cm*molecule^{-1})[62]. The deposition rate was obtained by recording infrared spectra at different times during the first hour of ice formation. Using bands between 3612 and 3003 cm^{-1}, 1047 and 1006 cm^{-1}, and 1192 and 1084 cm^{-1} for H_2O, CH_3OH, and NH_3, abundances were estimated at each time, and the slope for each molecule gave the deposition rate. The apparent irradiation rate was obtained by dividing the deposition rate by the photon flux of the UV lamp. Table 1 summarizes ice compositions, the apparent irradiation rate (T) and the deposition rate estimated previously. Once the photoprocessed ice is formed, the chamber is isolated from the turbo-molecular pumps and the cooling system is switched off, leading to an average heating rate of 2 K/min up to room temperature to obtain VOCs desorption. VOCs are then transferred to the GC-FT-Orbitrap-MS by adding ultrapure argon (Linde Ar 6.0) in the chamber to obtain a total pressure of 200 mbar. VOCs are preconcentrated in a specific interface in a 2.5-mL stainless steel tube cooled at 77 K with liquid nitrogen. Once recovered, the tube is warmed up and helium is added to a total pressure of 100 mbar. The resulting VOCs/helium gas mixture is then transferred to the injection unit of the GC that is formed by a stainless injection loop of 500 µL at 10^{-2} mbar. Once filled out, the gas sample is driven with helium to GC injector. Additional information can be obtained in the following refs. 60,63. Control experiments were performed to evaluate possible contamination coming from the experimental set-up: one consisting in depositing ice at 77 K without irradiation, and another one performing irradiation at 77 K without ice deposition (Fig. S17).

GC-FT-Orbitrap-MS configuration

The GC-MS analysis program is identical to the one used in ref. 64. The chosen chromatographic column is Rxi-624-Sil MS from Restek (60 m × 0.25 mm × 1.4 µm). The helium flow rate (Linde-France Scientific 6.0) is set at 1 mL/min with a vacuum compensation, a purge flow rate of 5.0 mL/min and a split of 10.0 mL/min. The temperature in the oven was from 35 °C (3 min) up to 130 °C at 2 °C/min and finally reached 280 °C for 2 min at 30 °C/min. The transfer line and injectors are set at 280 °C while the ionization source is set at 250 °C with electrons accelerated to 70 eV. VOCs are first concentrated in a deactivated silicate column with a cryotrap from Frontier Lab[61].

Data treatment

To obtain the detection of peaks in the chromatogram and their quantification, TraceFinder 4.1 software was used with a signal-to-noise greater than three. The integrating area (R) of the ion of each peak was corrected with the blank corresponding to the GC-FT-Orbitrap-MS analysis of an empty preconcentration loop. Control experiments have indeed shown that contamination came from this part of the experimental set-up. That is why blanks were performed between each experiment, as well as three replicates per ice composition. The compounds detected are then tentatively identified by comparing the fragmentation mass patterns to a high-resolution mass database containing 150 VOCs. When the database is not matching the experimental mass spectra, the tentatively identified VOCs are classified in groups (CH, CHO, CHO_2, CHN or CHNO) by taking into account the high resolution of the Orbitrap giving stoichiometric formula for each ion. Furthermore, mass patterns of tentatively identified VOCs are compared to our database and the NIST database to tentatively identify common patterns in order to propose a possible identification, noted in italic in Table S1. Additional information on compound identifications are given in Supplementary Information (Figs. S15 and S16).

Data availability

The data underlying this article will be shared on request to the corresponding author.

Received: 3 June 2025; Accepted: 5 September 2025;

References

1. Henning, T. & Semenov, D. Chemistry in protoplanetary disks. *Chem. Rev.* **113**, 9016–9042 (2013).
2. Jørgensen, J. K., Belloche, A. & Garrod, R. T. Astrochemistry during the formation of stars. *Annu. Rev. Astron. Astrophys.* **58**, 727–778 (2020).
3. Dartois, E. et al. Spectroscopic Sizing of Interstellar Icy Grains with JWST. *Nat. Astron*. **8**, 359–367 (2024).
4. van Dishoeck, E. F. ISO spectroscopy of gas and dust: from molecular clouds to protoplanetary disks. *Annu. Rev. Astron. Astrophys.* **42**, 119–167 (2004).
5. Rubin, M. et al. On the origin and evolution of the material in 67P/Churyumov-Gerasimenko. *Space Sci. Rev.* **216**, 102 (2020).
6. Altwegg, K. et al. Prebiotic chemicals—amino acid and phosphorus—in the coma of Comet 67P/Churyumov-Gerasimenko. *Sci. Adv.* **2**, 1–6 (2016).
7. Poch, O. et al. Ammonium salts are a reservoir of nitrogen on a cometary nucleus and possibly on some asteroids. *Science* **367**, eaaw7462 (2020).
8. Elsila, J. E., Glavin, D. P. & Dworkin, J. P. Cometary glycine detected in samples returned by Stardust. *Meteor. Planet. Sci.* **44**, 1323–1330 (2009).
9. Glavin, D. P., Dworkin, J. P. & Sandford, S. A. Detection of cometary amines in samples returned by Stardust. *Meteorit. Planet. Sci.* **413**, 399–413 (2008).
10. Brownlee, D. E. et al. Stardust: comet and interstellar dust sample return mission. *J. Geophys. Res.* **108**, 8111 (2003).
11. Oba, Y., Takano, Y., Dworkin, J. P. & Naraoka, H. Ryugu asteroid sample return provides a natural laboratory for primordial chemical evolution. *Nat. Commun.* **14**, 3107 (2023).
12. Yabuta, H. et al. Macromolecular organic matter in samples of the asteroid (162173) Ryugu. *Science* **379,** eabn9057 (2023).
13. Hashiguchi, M. et al. The spatial distribution of soluble organic matter and their relationship to minerals in the asteroid (162173) Ryugu. *Earth Planets Sp.* **75**, 73 (2023).
14. Yokoyama, T. et al. Samples returned from the asteroid Ryugu are similar to ivuna-type carbonaceous meteorites. *Science* https://doi.org/10.1126/science.abn7850 (2023).
15. Danger, G. et al. Characterization of laboratory analogs of interstellar/cometary organic residues using very high resolution mass spectrometry. *Geochim. Cosmochim. Acta* **118**, 184–201 (2013).
16. Ruf, A. et al. Organosulfur compounds formed by sulfur ion bombardment of astrophysical ice analogs: implications for moons, comets, and Kuiper belt objects. *Astrophys. J.* **885**, L40 (2019).
17. Henderson, B. L. & Gudipati, M. S. Direct detection of complex organic products in ultraviolet (Lyα) and electron-irradiated astrophysical and cometary ice analogs using two-step laser ablation and ionization mass spectrometry. *Astrophys. J.* **800**, 66 (2015).
18. Muñoz Caro, G. M. & Schutte, W. A. UV-photoprocessing of interstellar ice analogs: new infrared spectroscopic results. *Astron. Astrophys*. https://doi.org/10.1051/0004-6361:20031408 (2003).
19. Ruf, A. & Danger, G. Network analysis reveals spatial clustering and annotation of complex chemical spaces: application to astrochemistry. *Anal. Chem*. https://doi.org/10.1021/acs.analchem.2c01271 (2022).
20. Danger, G. et al. Insight into the molecular composition of laboratory organic residues produced from interstellar/pre-cometary ice analogues using very high resolution mass spectrometry. *Geochim. Cosmochim. Acta* **189**, 184–196 (2016).
21. Öberg, K. I. Photochemistry and astrochemistry: photochemical pathways to interstellar complex organic molecules. *Chem. Rev.* **116**, 9631–9663 (2016).
22. Theule, P. et al. Thermal reactions in interstellar ice: a step towards molecular complexity in the interstellar medium. *Adv. Sp. Res.* **52**, 1567–1579 (2013).
23. Fresneau, A. et al. Cometary materials originating from interstellar ices: clues from laboratory experiments. *Astrophys. J.* **837**, 168 (2017).
24. Fresneau, A. et al. Trapping in water—an important prerequisite for complex reactivity in astrophysical ices: the case of acetone (CH_3) 2C=O and ammonia NH_3. *Mon. Not. R. Astron. Soc.* **443**, 2991–3000 (2014).
25. Öberg, K. I. et al. Formation rates of complex organics in UV irradiated CH3OH-rich ices I: experiments. *Astron. Astrophys.* **504**, 891 (2009).
26. Yocum, K. M., Milam, S. N., Gerakines, P. A. & Widicus Weaver, S. L. Sublimation of laboratory ices millimeter/submillimeter experiment (SubLIME): structure-specific identifications of products from UV-photolyzed methanol ice. *Astrophys. J.* **913**, 61 (2021).
27. Abou Mrad, N., Duvernay, F., Isnard, R., Chiavassa, T. & Danger, G. The gaseous phase as a probe of the astrophysical solid phase chemistry. *Astrophys. J.* **846**, 124 (2017).
28. Tenelanda-Osorio, L. I. et al. Effect of the UV dose on the formation of complex organic molecules in astrophysical ices: irradiation of methanol ices at 20 K and 80 K. *Mon. Not. R. Astron. Soc.* **515**, 5009–5017 (2022).
29. Singh, S. K., Zhu, C., La Jeunesse, J., Fortenberry, R. C. & Kaiser, R. I. Experimental identification of aminomethanol (NH_2CH_2OH)—the key intermediate in the Strecker synthesis. *Nat. Commun.* **13**, 375 (2022).
30. Dartois, E. The ice survey opportunity of ISO. *Space Sci. Rev.* **119**, 293–310 (2005).
31. Ciesla, F. J. & Sandford, S. A. Organic synthesis via irradiation and warming of ice grains in the solar nebula. *Science* **336**, 452–454 (2012).
32. Abou Mrad, N., Duvernay, F., Chiavassa, T. & Danger, G. Methanol ice VUV photo-processing: GC-MS analysis of volatile organic compounds. *Mon. Not. R. Astron. Soc.* **458**, 1234–1241 (2016).
33. Turner, A. M. et al. A photoionization mass spectrometry investigation into complex organic molecules formed in interstellar analog ices of

carbon monoxide and water exposed to ionizing radiation. *Astrophys. J.* **916**, 74 (2021).
34. Gutiérrez-Quintanilla, A. et al. ICOM formation from radical chemistry: a mechanistic study from cryogenic matrix coupled with IR and EPR spectroscopies. *Mon. Not. R. Astron. Soc.* **506**, 3734–3750 (2021).
35. De Marcellus, P. et al. Aldehydes and sugars from evolved precometary ice analogs: importance of ices in astrochemical and prebiotic evolution. *Proc. Natl. Acad. Sci. USA* **112**, 965–970 (2015).
36. Gautier, T. et al. Laboratory experiments to unveil the molecular reactivity occurring during the processing of ices in the protosolar nebula. *Earth Planet. Sci. Lett.* **531**, 116011 (2020).
37. Kim, Y. S., Bennett, C. J., Chen, L.-H., O'Brien, K. & Kaiser, R. I. Laboratory studies on the irradiation of solid ethane analog ices and implications to Titan's chemistry. *Astrophys. J.* **711**, 744–756 (2010).
38. Jackson, W. M., Faris, J. & Buccos, N. J. Vacuum-ultraviolet photolysis of ethane films. *J. Chem. Phys.* **45**, 4145–4148 (1966).
39. Scheer, M. D., McNesby, J. & Klein, R. Vacuum photolysis of solid ethane at 77° K. *J. Chem. Phys.* **36**, 3504–3505 (1962).
40. Qasim, D. et al. Formation of interstellar propanal and 1-propanol ice: a pathway involving solid-state CO hydrogenation. *Astron. Astrophys.* **627**, A1 (2019).
41. Zheng, W., Jewitt, D., Osamura, Y. & Kaiser, R. I. Formation of nitrogen and hydrogen-bearing molecules in solid ammonia and implications for solar system and interstellar ices. *Astrophys. J.* **674**, 1242–1250 (2008).
42. Zins, E. L. & Krim, L. Formation and characterization of VUV photolytically-induced (NH_2)(NH3)n aggregates, $0 \leq n \leq 3$. *RSC Adv.* **3**, 10285 (2013).
43. Lamberts, T., Markmeyer, M. N., Kolb, F. J. & Kästner, J. Formation of acetaldehyde on CO-rich ices. *ACS Earth Sp. Chem.* **3**, 958–963 (2019).
44. Enrique-Romero, J. et al. Revisiting the reactivity between HCO and CH3 on interstellar grain surfaces. *Mon. Not. R. Astron. Soc.* **493**, 2523–2527 (2020).
45. Oberg, K. I. et al. The effect of H_2O on ice photochemistry. *Astrophys. J.* **718**, 832–840 (2010).
46. Krim, L., Lasne, J., Laffon, C. & Parent, P. Influence of water in the UV-induced chemistry of methanol in the solid phase. *J. Phys. Chem. A* **113**, 8979–8984 (2009).
47. Loeffler, M. J. & Hudson, R. L. Descent without modification? The thermal chemistry of H_2O_2 on Europa and other icy worlds. *Astrobiology* **15**, 453–461 (2015).
48. Bennett, C. J. & Kaiser, R. I. On the formation of glycolaldehyde ($HCOCH_2OH$) and methyl formate ($HCOOCH_3$) in interstellar ice analogs. *Astrophys. J.* **661**, 899–909 (2007).
49. Bennett, C. J., Chen, S., Sun, B., Chang, A. H. H. & Kaiser, R. I. Mechanistical studies on the irradiation of methanol in extraterrestrial ices. *Astrophys. J.* **660**, 1588–1608 (2007).
50. Kim, Y. S. & Kaiser, R. I. On the formation of amines (Rnh 2) and the cyanide anion (Cn –) in electron-irradiated ammonia-hydrocarbon interstellar model ices. *Astrophys. J.* **729**, 68 (2011).
51. Suzuki, T. et al. Survey of CH_3 NH_2 and its formation process. *Astrophys. J.* **954**, 189 (2023).
52. Förstel, M., Bergantini, A., Maksyutenko, P., Góbi, S. & Kaiser, R. I. Formation of methylamine and ethylamine in extraterrestrial ices and their role as fundamental building blocks of proteinogenic α-amino acids. *Astrophys. J.* **845**, 83 (2017).
53. Canta, A., Öberg, K. I. & Rajappan, M. The formation of imines and nitriles during VUV photoirradiation of NH_3:C_2Hx ice mixtures. *Astrophys. J.* **953**, 81 (2023).
54. Vinogradoff, V. et al. Importance of thermal reactivity for hexamethylenetetramine formation from simulated interstellar ices. *Astron. Astrophys.* **551**, A128 (2013).
55. Danger, G. et al. Experimental investigation of nitrile formation from VUV photochemistry of interstellar ices analogs: acetonitrile and amino acetonitrile. *Astron. Astrophys.* **525**, A30 (2011).
56. Theulé, P. et al. Kinetic studies on low-temperature solid-state reactions in interstellar ices. *EAS Publ. Ser.* **58**, 363–367 (2013).
57. Danger, G. et al. Experimental investigation of aminoacetonitrile formation through the Strecker synthesis in astrophysical-like conditions: reactivity of methanimine (CH_2NH), ammonia (NH_3), and hydrogen cyanide (HCN). *Astron. Astrophys.* **535**, A47 (2011).
58. Gautier, T. et al. Development of HPLC-Orbitrap method for identification of N-bearing molecules in complex organic material relevant to planetary environments. *Icarus* **275**, 259–266 (2016).
59. Nuevo, M. et al. Enantiomeric separation of complex organic molecules produced from irradiation of interstellar/circumstellar ice analogs. *Adv. Sp. Res.* **39**, 400–404 (2007).
60. Abou Mrad, N., Duvernay, F., Chiavassa, T. & Danger, G. Methanol ice VUV photo-processing: GC-MS analysis of volatile organic compounds. *Mon. Not. R. Astron. Soc.* **458**, 1234 (2016).
61. Abou Mrad, N., Werner, S., Mouzay, J. & Danger, G. Sensitivity and resolution optimization in gas chromatography coupled to mass spectrometry analyses of volatile organic compounds present in vacuum environment. *J. Chromatogr. A* **1609**, 460489 (2020).
62. Bouilloud, M. et al. Bibliographic review and new measurements of the infrared band strengths of pure molecules at 25 K: H_2O, CO_2, CO, CH_4, NH_3, CH_3OH, HCOOH and H_2CO. *Mon. Not. R. Astron. Soc.* **451**, 2145–2160 (2015).
63. Abou Mrad, N., Duvernay, F., Theulé, P., Chiavassa, T. & Danger, G. Development and optimization of an analytical system for volatile organic compound analysis coming from the heating of interstellar/cometary ice analogues. *Anal. Chem.* **86**, 8391–8399 (2014).
64. Javelle, T., Righezza, M. & Danger, G. Identify low mass volatile organic compounds from cometary ice analogs using gas chromatography coupled to an Orbitrap mass spectrometer associated to electron and chemical ionizations. *J. Chromatogr. A* **1652**, 462343 (2021).

Acknowledgements

The research was funded by the Centre National d'Etudes Spatiales (CNES, R-S18/SU-0003-072 and R-S18/SU-0003-072, PI: G.D.), and the Centre National de la Recherche Française (CNRS) with the programs "Physique et Chimie du Milieu Interstellaire" (PCMI-PI: G.D.) and "Programme National de Planétologie" (PNP) (PI: G.D.). G.D. is grateful to the Agence Nationale de la Recherche for funding via the ANR RAHIIA_SSOM (ANR-16-CE29-0015) and VAHIIA (ANR-12-JS08-0001). The project has further received funding from the EXCellence Initiative of Aix-Marseille Université - A*Midex, a French "Investissements d'Avenir programme" AMX-21-IET-018, and from the Région SUD Provence Alpes Côte d'Azur "Apog 2017" – PILSE. Furthermore, funded by the Deutsche Forschungsgemeinschaft (DFG, German Research Foundation) under Germany's Excellence Strategy - EXC 2094 - 390783311 (A.R.).

Author contributions

G.D. and T.J. defined the working flow of this study. T.J. performed ice processing. C.G. and T.J. developed protocols for GC-MS analyses. G.D., C.G., T.J., A.R., and L.S. worked on data treatments. F.D., G.D., and T.J. elaborate the reactivity scheme. All authors discussed the results and commented on the manuscript.

Competing interests

The authors declare no competing interests.

Additional information

Supplementary information The online version contains supplementary material available at https://doi.org/10.1038/s42004-025-01692-y.

Correspondence and requests for materials should be addressed to Grégoire Danger.

Peer review information *Communications Chemistry* thanks the anonymous reviewers for their contribution to the peer review of this work. A peer review file is available.

Reprints and permissions information is available at http://www.nature.com/reprints

Publisher's note Springer Nature remains neutral with regard to jurisdictional claims in published maps and institutional affiliations.

Open Access This article is licensed under a Creative Commons Attribution-NonCommercial-NoDerivatives 4.0 International License, which permits any non-commercial use, sharing, distribution and reproduction in any medium or format, as long as you give appropriate credit to the original author(s) and the source, provide a link to the Creative Commons licence, and indicate if you modified the licensed material. You do not have permission under this licence to share adapted material derived from this article or parts of it. The images or other third party material in this article are included in the article's Creative Commons licence, unless indicated otherwise in a credit line to the material. If material is not included in the article's Creative Commons licence and your intended use is not permitted by statutory regulation or exceeds the permitted use, you will need to obtain permission directly from the copyright holder. To view a copy of this licence, visit http://creativecommons.org/licenses/by-nc-nd/4.0/.

© The Author(s) 2025, corrected publication 2025